A novel transient infrared imaging method for non-intrusive, low-cost, fast, and accurate air leakage detection in building envelopes

Tianli Feng [a,*], Zhenglai Shen [b], Som S. Shrestha [b], Diana E. Hun [b]

[a] *Department of Mechanical Engineering, University of Utah, Salt Lake City, UT, 84112, USA*
[b] *Buildings and Transportation Science Division, Oak Ridge National Laboratory, Oak Ridge, TN, 37831, USA*

ARTICLE INFO

ABSTRACT

Air leakage through the building envelope in the U.S. accounts for about four quads of energy annually, costing approximately $40 billion per year. However, a high-fidelity and non-intrusive method to detect air leakage has not been demonstrated to date. In this paper, we propose a novel non-intrusive and low-cost method called Transient Infrared (IR) Imaging (TIRI) that can rapidly and accurately identify air leakage locations and relative rates on building envelopes. When the interior and exterior temperatures are different, and a small internal pressure pulse is created by HVAC, the temperature at locations with air leakages will change rapidly, while the areas without a leakage do not change. Based on a heat transfer model, we have derived the temperature change as a function of time after the HVAC is turned on. By tracking the temperature change, which depends on leakage rate and size, we have obtained the air leakage map in the case studies. Using an exterior door as an example, we took transient IR images in different seasons and different times of the day, and successfully obtained the leakage map in all the scenarios. Successfully obtained the air leakage map even when the indoor-outdoor air temperature difference is as small as 2 °C. We have also realized a detection speed of 10s and demonstrated that this method also worked for windows, which have mirror-like IR reflections. Our TIRI method will accelerate the improvement of airtightness in buildings, save building energy, and help reduce greenhouse gas emissions.

1. Introduction

Buildings represent the most substantial energy consumption sector in the United States [1] and the European Union [2], accounting for approximately 40 % of annual primary energy usage. Notably, within the realm of building energy consumption, nearly half is attributed to the heating, ventilation, and air conditioning (HVAC) systems, and air leakage is estimated to contribute to 30–50 % of the HVAC loads [3]. Detection and sealing air leakage has the potential to conserve four quadrillion BTUs of energy annually in the USA, equivalent to approximately $40 billion [4]. Additionally, the flow of moisture-laden air can compromise the durability of materials and promote the growth of mold and mildew within the building envelope [4,5].

Many methods have been developed and tested for building air leakage detection over the past four decades [6]. Among them, the blower door test is the most widely used method [7], which employs a specialized fan temporarily mounted to an exterior doorway

---

* Corresponding author.
E-mail address: tianli.feng@utah.edu (T. Feng).

frame. Once properly calibrated, this powerful fan can modulate the interior air pressure by either expelling or introducing air. As a result, air infiltrates or exfiltrates through all unsealed gaps, cracks, and openings. Additionally, a harmless smoke pencil can be employed to pinpoint air leaks [8,9]. The resultant data, representing the home's air leakage rate, is captured on a digital device. During the test, infrared cameras can also be utilized to identify insulation voids and air leakage points [10,11]. Hart provided a general guide on employing infrared thermography for diagnosing buildings in 1992 [12]. Hart pointed out that this method is not accurate, requires many parameters, needs a minimal indoor-outdoor temperature difference of 5 °C, and relies on environmental conditions. Another notable contribution to this field was made by Grinzato et al. who employed IR cameras to identify defective areas on building envelope [13]. Their approach involved solving the transient heat transfer equation under periodic or pulsed heating [13]. However, this method is complex and was not employed widely. Besides, many IR-based methods have been explored based on various models [11,14–20]. Nevertheless, all of them rely on depressurization or pressurization fans to induce indoor-outdoor pressure difference (50–75Pa) or temperature differences (10 °C) [6]. Furthermore, these methods mainly focus on static IR images, which need complex heat transfer models and many parameters to fit the model in order to detect air leakage. The presence of thermal bridging can further complicate the process by affecting the contrast and making it challenging to pinpoint the exact location of air leakage. Exterior imaging is also susceptible to external factors like weather, wind, and buoyancy flow, while interior imaging can be affected by the presence of furniture and decorations. Active IR imaging proposed by Lerma et al. [21] is a transient method, but they rely on a 2500 W IR lamp to heat up the leaking spot, which is costly and intrusive. The alternative non-IR related methods, such as low-frequency acoustical monopole [22], anemometer, smoke canister [23], micro-electromechanical pressure sensors [24], microphone arrays [25–29], sound reduction index monitoring [30], and refractive index optical imaging [31], either are costly, intrusive or have a low signal-to-noise ratio (accuracy) due to the small temperature and pressure variations and the considerable interference posed by external environment and complex geometry envelop. Overall, a high-fidelity and non-intrusive method has not been demonstrated to date [6].

In this paper, we present a simple and novel method that utilizes the time evolution of IR images under a small pressure pulse created by HVAC systems to identify both the locations and relative rates of air leakage, without the need for pressurization fans. While Hart previously discussed the use of infrared thermography to detect air leakage by monitoring the expansion of cold areas during the depressurization process, it is important to note that the method still relies on mechanical extraction fans, and no tests were done then [12]. Additionally, although recent literature has explored time-dependent IR images, they have primarily been used to monitor the surface temperature change over a long period (e.g., 30 min to reach a steady state) to study the effects of pressure rather than transiently detecting air leakage [11]. The remainder of the manuscript is organized as follows. In Section 2, we introduce the developed new method. In Section 3, we demonstrate the feasibility of the new method on a testing door and window. In Section 4, we demonstrate the imaging processing method and demonstrate the generation of air leakage maps. In Sections 5 and 6, we demonstrate our method in various conditions. Section 7 provides an outlook, and Section 8 draws conclusions.

2. Theoretical methodology

Instead of analyzing the static IR images, we propose a novel technique called transient IR imaging or "TIRI", which involves analyzing time-dependent IR images. We assume the interior of a building is maintained at a given temperature (for example, 23 °C), and the outdoor air is at a different temperature (being either higher or lower than 23 °C). When the building's HVAC system undergoes operational changes, such as turning on or off or changing the blower speed, the air leakage rates at the locations with cracks,
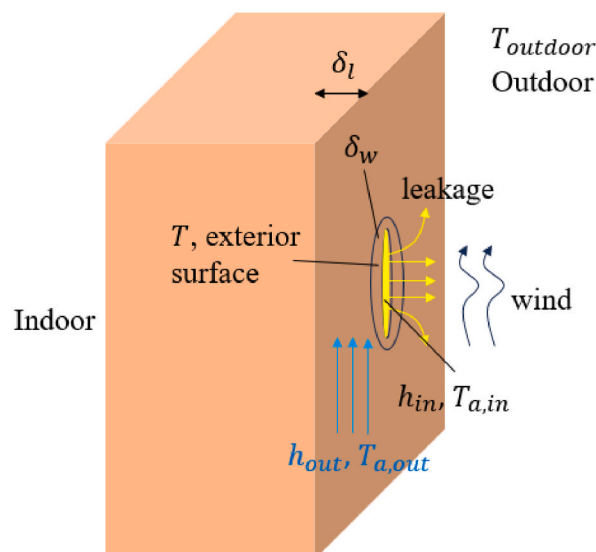

Fig. 1. Sketch of the heat transfer processes around the exterior surface of a crack.

gaps, or openings will change immediately due to the sudden pressure pulse induced by HVAC. Immediately after the change of HVAC operation happens, the locations with air leakage should have a noticeable temperature change over time (within ~minutes) due to the convection airflow through the leakage spots. In contrast, the locations without leakage should not experience a temperature change. Therefore, we propose that by taking the transient IR images over time and tracking the temperature change at various locations, we can identify the locations of air leakage.

The TIRI method can effectively distinguish thermal bridges from leakages. Thermal bridges exhibit temperature patterns similar to those of air leakage locations in static IR images, making it hard to differentiate between the two in the conventional IR imaging methods. However, the TIRI method offers an effective means to distinguish them by focusing on tracking the temperature changes (relative temperature) rather than the absolute temperature. The thermal bridge location's temperature should stay constant after the change of HVAC operation happens. In contrast, leakage locations' temperature should change rapidly.

Fig. 1 shows a crack on a building's exterior wall and its simplified model. In the TIRI method, after the HVAC is turned on, the surface temperature close to the crack is controlled by the heat transfer equation:

$$P\delta_l\delta_w \cdot \rho c \frac{\partial T}{\partial t} = h_{in}\delta_l P\left(T_{a,in} - T\right) + h_{out}\delta_w P\left(T_{a,out} - T\right) - kP\delta_l \frac{\partial^2 T}{\partial r^2} \tag{1}$$

Here, P is the perimeter of the crack cross section. δ_w is the width of the tiny area of interest near the crack. δ_l is a small portion of wall thickness of interest near the exterior surface. $T_{a,in}$ is the temperature of the air inside the crack near the exterior surface. h_{in} is the air convection coefficient inside the crack. $T_{a,out}$ is the air temperature for the external convection of the surface surrounding the crack (i.e., the annular band-shaped area shaded in the diagram). $T_{a,out}$ is a mixture of the outdoor air and the air flowing out from the crack. The value of $T_{a,out}$ depends on the wind speed and leaking speed and but should be in between $T_{a,in}$ and $T_{outdoor}$. h_{out} is the convection coefficient on the exterior surface near the crack, which depends on the outdoor wind. T is the temperature of the exterior area around the crack that is to be measured by the TIRI. ρ, c, k are the density, heat capacity, and thermal conductivity of the exterior wall.

The first term in Eq. (1) is the energy change rate of the control volume studied around the crack. The second term is the heat gained by convection from leaking air inside the crack. The third term is the heat gained by convection from the exterior surface. The last term is the heat loss due to conduction inside the wall. Radiation is ignored since it is small compared to conduction and convection during a short time. During the short time of TIRI, we assume the conduction is neglected, compared to convection, and Eq. (1) is reduced to

$$\rho c \frac{\partial T}{\partial t} = A - BT \tag{2}$$

where

$$A = \frac{h_{in}}{\delta_w}T_{a,in} + \frac{h_{out}}{\delta_l}T_{a,out} \tag{3}$$

$$B = \frac{h_{in}}{\delta_w} + \frac{h_{out}}{\delta_l} \tag{4}$$

The solution to Eq. (2) is an exponential function as follows:

$$T = \left(T_0 - \frac{A}{B}\right)e^{-\frac{B}{\rho c}t} + \frac{A}{B} \tag{5}$$

At time 0, the exterior surface temperature is T_0. After a long time, the temperature gradually approaches the final steady-state temperature A/B, which is not the interest of our work. In the TIRI method, we are only interested in very short time after time 0. Within a short time (small t), the exponential function can be approximated by a linear function:

$$T = T_0 + \frac{B}{\rho c}\left(\frac{A}{B} - T_0\right)t, (t \text{ is small}) \tag{6}$$

which indicates that the exterior surface temperature should change linearly after turning on the HVAC system, and the temperature change rate is

$$\frac{dT}{dt}\Big|_{\text{short } t} = \frac{B}{\rho c}\left(\frac{A}{B} - T_0\right) \tag{7}$$

Here, for simplicity, we assume $h_{in} \sim h_{out}$ and $\delta_l \sim \delta_w$, and Eq. (7) can be reduced to

$$\frac{dT}{dt}\Big|_{\text{short } t} \approx \frac{h_{in} + h_{out}}{\rho c \delta}\left(\frac{T_{a,in} + T_{a,out}}{2} - T_0\right) \tag{8}$$

Here h_{in} and h_{out} are very complex and dependent on many factors. For example, a rougher, narrower, and more winding crack should have higher friction, lower air flow speed, and lower convection coefficient near the exit (h_{in}). h_{out} depends on leaked air flow rate and the outdoor wind speed and direction. $T_{a,in}$ depends on the crack length and roughness. $T_{a,out}$ is the temperature of the mixed air that consists of leaked air and outdoor air, and depends on the air leaking rate and wind speed. Higher leaking rate can bring $T_{a,out}$ closer to

$T_{a,in}$, which will increase the absolute value of dT/dt. It is unlikely to find the exact analytical expression of h_{in}, h_{out}, $T_{a,in}$, and $T_{a,out}$, which is also not the focus of this work. As a rule of thumb, h_{in} can be roughly approximated by the fully-developed turbulent flow in a rough tube [32–34],

$$h_{in} = \frac{k_{air}}{D} \text{Nu}_D \sim \frac{k_{air}}{D} \text{Re}_D^{\frac{4}{5}} \text{Pr}^n \sim \frac{k_{air}\rho_{air}^{4/5}\text{Pr}^n}{D^{\frac{1}{5}}\mu^{\frac{4}{5}}} v_{air}^{4/5} \tag{9}$$

Here, Nu_D, Re_D, and Pr are the Nusselt, Reynolds, and Prandtl numbers of air, respectively. μ, v_{air}, ρ, k_{air} are the dynamic viscosity, velocity, density, and thermal conductivity of air leaking out from the crack. D is the diameter of the crack. The exponent 4/5 is written as 0.78–1 in the literature for different types of rough tubes [32–34], and we take 4/5 just as a first order approximation. Equations (6)–(9) indicate that the temperature changes linearly with time in the TIRI regime, and the change rate is positively correlated to air leakage velocity and indoor-outdoor temperature difference, inversely proportional to wall density and heat capacity.

After collecting IR images, we will conduct a linear fitting of the temperature of each pixel, $T_i(t)$, as a function of time (t):

$$T_i(t) = K_i t + c_i \tag{10}$$

to obtain the temperature change rate $K_i = dT_i/dt$ of each pixel i. The air leakage map can be obtained by using the amplitudes of $|K_i|$. The brightness of each pixel represents the relative amplitude of $|K_i|$, or the relative leakage rate. Since the measured absolute temperature of different IR images may not be consistent due to the intrinsic limitations and fluctuations of the IR camera, we also propose to use a more advanced method to process the transient IR images using a normalized temperature rather than absolute temperatures. We define a normalized dimensionless temperature of each pixel, $T_i^*(t)$, as

$$T_i^*(t) \equiv \frac{T_i(t) - \overline{T}(t)}{\overline{T}(t)} \tag{11}$$

Here $T_i(t)$ is the temperature of the pixel i at time t, and $\overline{T}(t) = \frac{1}{N}\sum_{i=1}^{N} T_i(t)$ is the average temperature of all the pixels in one IR image at time t. For each time t, $T_i^*(t)$ represents the derivation of each pixel's temperature from the average pixel temperature. After fitting $T_i^*(t)$ as a linear function,

$$T_i^*(t) = K_i^* t + c_i^* \tag{12}$$

we can obtain the leakage map by plotting the amplitudes of $|K_i^*|$ as an image.

3. Case studies on an exterior door

3.1. Temperature as a function of time

We tested the TIRI method on a closed door of a residential building in February in Salt Lake City, UT, with an outdoor temperature of around 6 °C and an indoor temperature of 24 °C. The IR camera used was the FLIR T420, which is a common medium level IR camera with 320 × 240 pixels. There is no special requirement for the camera. We expect the TIRI method to work for general IR cameras, and the spatial resolution depends on the camera itself. As shown in Fig. 2, the camera was placed about 1.2 m from the door, and 0.8 m from the floor. The height and angle do not matter significantly as long as the camera focuses on the detected area. The IR video was recorded at 1 fps for 22 min with the HVAC status: off initially, on at 1 min, off at 10 min, on again at 14 min, and finally off at 18 min. The wind speed was monitored by an anemometer. The temperatures of the leaking spot and two references points as a function of
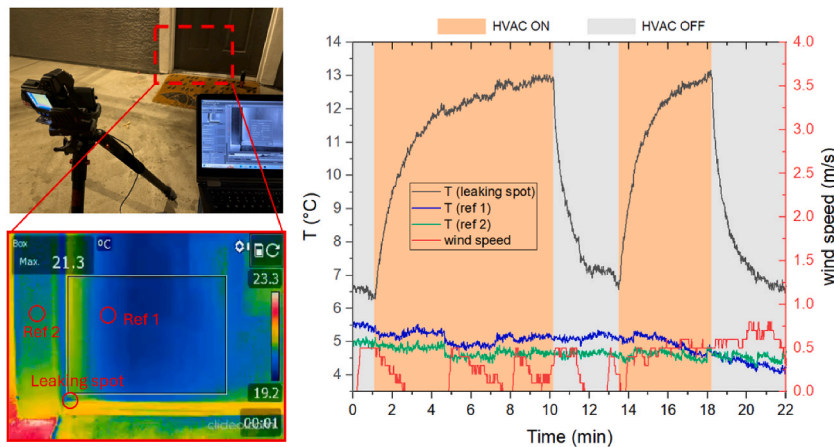

Fig. 2. Case study of the TIRI method on a door in Salt Lake City. The locations with air leakage showed clear temperature change while the locations without air leakage remained at a constant temperature during the operational change of HVAC.

temperature are shown in Fig. 2. Clearly, the leaking spot temperature changed rapidly with time as the HVAC was turned on or off, while the temperatures of the non-leaking spots remained nearly constant.

When the HVAC was first turned on, the temperature of the leaking spot rose linearly within 2 min. Any time frame within this 2-min window can be used to detect and quantify air leakage. After 10 min, the spot gradually saturated to the maximum temperature that it could reach. This approaching speed is an exponential function, which is consistent with our model solution, Eq. (5). When we turned off the HVAC, the leaking spot rapidly cooled back to its original temperature, also in an exponential decay format, consistent with Eq. (5). Before the experiment, it was expected that the cooling curve following HVAC OFF is symmetric to the heating curve following HVAC ON. However, we found that the time spent for cooling back was much shorter than that spent for heating up. This is understandable because the detected spot is on the exterior wall rather than the interior wall, and therefore, the speed of cooling back to environment is faster. After that, we turned on/off the HVAC once again and found that the temperature curve was similar. With that being said, both directions (i.e., turning HVAC on and off) can be used for air leakage detection, providing more flexibility and efficiency for practical applications. It is noted that, whenever there was a strong wind, the temperature change slop decreased remarkably. This also agrees with our model, Eq. (8), i.e., the temperature change rate depends on the external heat convection coefficient. The impact of wind speed is only discussed qualitatively in this work. Future studies are expected to be conducted to comprehensively quantify the leaking rate in various environments.

3.2. Processing of TIRI images to obtain leakage map

With the transient IR images, we are able to obtain the leakage map. The temperature change rate, or dT/dt, of each pixel in the IR image series can be viewed as an indicator of the leakage rate. By tracking the change of a series of IR images, we can also effectively eliminate the disturbance caused by thermal bridges and different materials' emissivity. Fig. 3 shows the results after processing five IR images taken at an interval of 10 s after the HVAC was turned on. We conducted a linear fitting of the temperature of each pixel $T_i(t)$ as a function of time and obtained the temperature change rate, $K_i = dT_i/dt$, for each pixel i. Fig. 3 (b) shows the amplitudes of $|K_i|$ of all the 320×240 pixels, which is an air leakage map. The brightness of each pixel represents the relative amplitude of $|K_i|$, or the relative leakage rate. Here, to eliminate the noise and increase the signal-to-noise ratio, we have eliminated the pixels that show a negative K_i value or a K_i value smaller than the fitting error. It is seen that the processed TIRI image can clearly show the leakage locations and relative rates by using only five images (taken within 40 s). We have also tested using the normalized temperature $T_i^*(t)$ and plotted the amplitudes of $|K_i^*|$ as an image shown in Fig. 3 (c), which shows a similar accuracy to Fig. 3 (b). This indicates that the IR measurement is stable and consistent throughout the five IR images. In order to determine the shortest time needed to detect leakage, we took another video with 30 fps for 10s. As shown in Fig. 4, the leaking spot has a clear temperature increasing trend, compared to the non-leaking spot even within 10s. The obtained leak map using the 10s data can clearly identify the leaking area. When further shortening the time to 5s, we find that it can still obtain a good leak map, but with a bit larger noise. This is because the natural temperature fluctuation of each frame overwhelms the overall temperature change trend.

4. Case studies in different seasons and weathers

To test whether the TIRI method also works in the summer season, we have conducted another set of tests in July in Salt Lake City when the outdoor temperature is 36 °C. It is well accepted that leakage is much less serious in summer compared to winter due to thermal expansion. Using either ten or five IR images, we have successfully obtained a clear air leakage map, as shown in Fig. 5. Interestingly, we find that the leakage at Location 5 seen in the winter in Fig. 3 disappear in Fig. 5. This is because the door is thermally expanded in the summer and sealed on the edge. This is also why air leakage is more serious in the winter than summer. This again demonstrates the broad applicability of our TIRI method. We have also tested using absolute temperature instead of normalized temperature and obtained similar results, which are not shown here redundantly.

To further test the limit of our TIRI method, we conducted more experiments at different outdoor temperatures. As shown in Fig. 6, we have done independent tests with outdoor temperatures of 31, 29, 28, and 26 °C. Surprisingly and inspiringly, we find that the TIRI method can effectively detect air leakage even with a small indoor-outdoor temperature difference of 2 °C. This is because the TIRI method only relies on the relative temperature change rather than the absolute temperature. Even though IR cameras have an intrinsic temperature measurement accuracy, often in the order of 2–3 °C depending on the emissivity of the surface, our method can detect
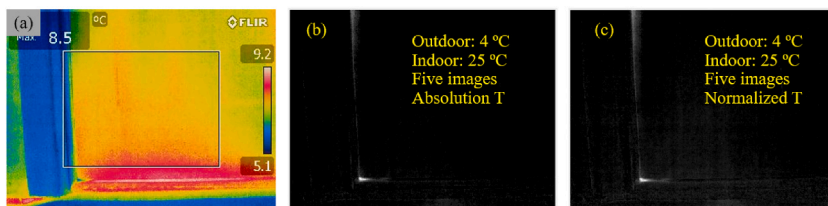

Fig. 3. Testing of the TIRI method on a closed door of a residential building in Salt Lake City in winter with an outdoor temperature of 4 °C. (a) An IR image. (b, c) The obtained air leakage maps were processed by using five IR images in a row with 10 s interval between each two images. The brightness represents the relative air leakage rates. In (b), the brightness is proportional to the absolute temperature change rate. In (c), the brightness is proportional to the normalized temperature change rate. Note that the outdoor temperature mentioned in this paper and labeled in the figures is the outdoor air temperature instead of the exterior wall surface temperature or the measured temperature by the IR camera.
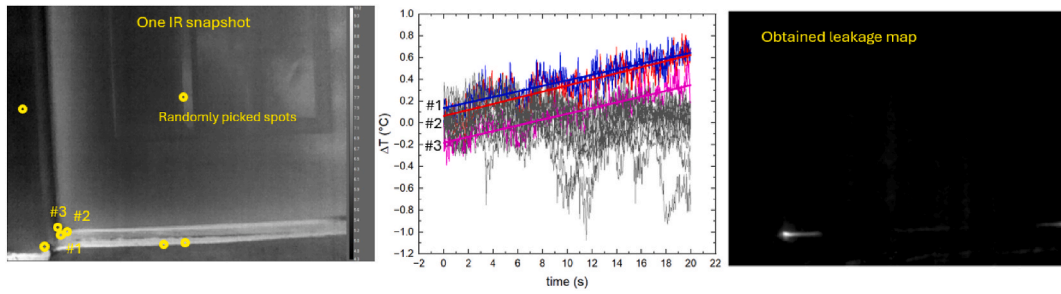
Fig. 4. Testing of the TIRI method with 30 fps for 10s on a closed door of a residential building in Salt Lake City in winter with an outdoor temperature of 4 °C.
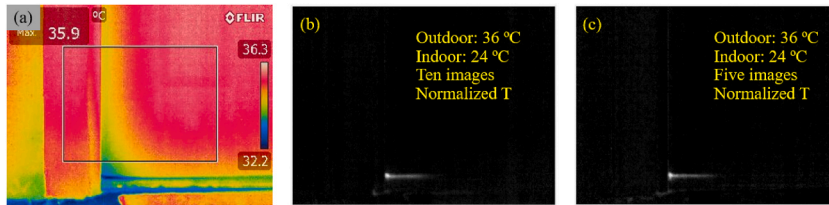

Fig. 5. Testing of the TIRI method on a closed door of a residential building in Salt Lake City in a summer with an outdoor temperature of 36 °C. (a) An IR image. (b, c) The obtained air leakage maps were processed by using ten (b) and five (c) IR images in a row.
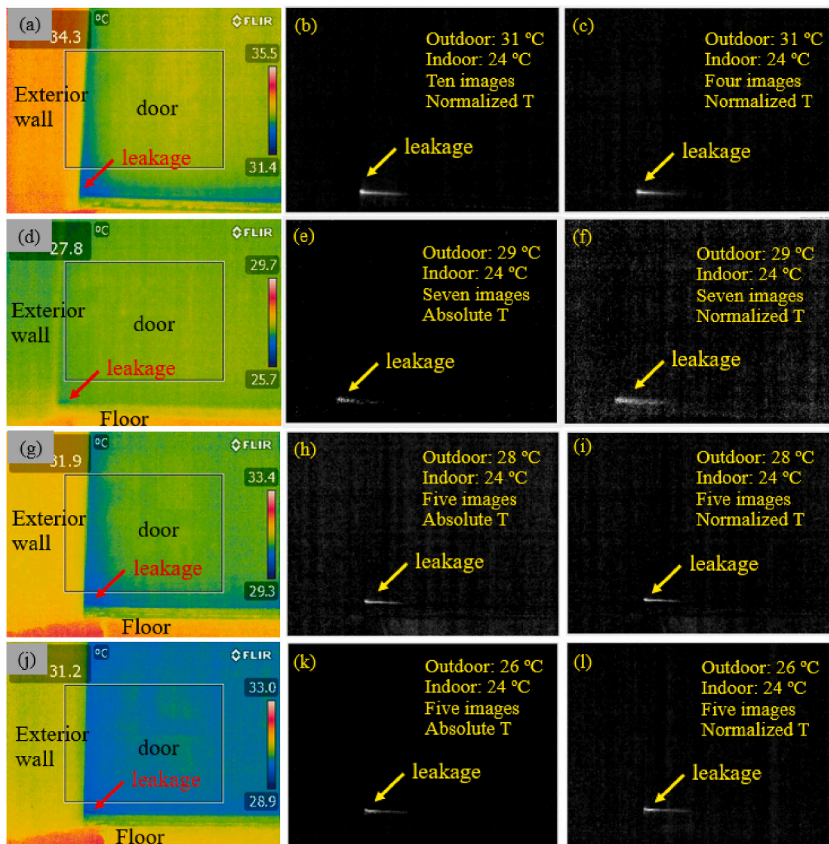

Fig. 6. Testing of the TIRI method on a closed door of a residential building in Salt Lake City at the outdoor temperature of (a–c) 31 °C, (d–f) 29 °C, (g–i) 28 °C, and (j–l) 26 °C. Note that the "outdoor temperature" is the outdoor air temperature, which is different from the exterior wall temperature or the temperature given by the IR camera.

temperature below 0.1 °C. Even if the IR camera does not measure the absolute temperature accurately, it does not affect the accuracy of the TIRI method as long as the IR images were taken using the same IR camera. We note that using the normalized temperature gradient can obtain better results than using the absolute temperature gradient when the indoor-outdoor temperature difference is small, as shown in Fig. 6(e and f). This is because the normalization of temperature can eliminate the small temperature fluctuation intrinsically caused by the camera.

5. Case studies on a window

Since glass usually has mirror-like IR reflectance and is extremely hard to measure using IR cameras, we conducted a case study of TIRI on a window of a residential building, as shown in Fig. 7. The test was done in February in Salt Lake City, UT, with an outdoor temperature of around 0 °C and indoor temperature of around 24 °C. The window was opened with a 1-mm slit for testing, as shown in Fig. 7 (b). After turning on the HVAC at time = 0, IR images were taken every 10 s. As shown in Fig. 7 (a), it is difficult to observe the temperature changes from the IR images using the naked eye. However, after extracting the temperature data as a function of time, it is clearly seen the different temperature changes at different locations in Fig. 7(c and d). The temperatures at Locations #2 and #3, which are near the slit, changed rapidly, while Locations #1 and #4 did not change.

We have also tested the TIRI method on a window at different outdoor temperatures. As seen in Fig. 8, the 1 mm open slit of the window can be clearly detected by the TIRI method. As a control experiment, the closed window does not show any air leakage in the obtained leakage map. Since glass has a mirror-like IR reflection, the temperature detected by IR camera of the window is not trustable. As seen in Fig. 8 (a), (d), and (g), the window reflects the IR light emitted by the iron railing and the tester. To resolve this issue, we have masked the glass area as shown in Fig. 8 and successfully obtained the leak map.

6. Case studies on a suspicious spot

Last, we tested TIRI on a suspicious area between the wall and floor, where a bright spot suggested the possibility of air leakage, as shown in Fig. 9. However, by taking the transient IR images after the HVAC was turned on, it was evident that the temperature of the spot did not change over time, indicating that the white spot was simply a thermal bridge rather than an air leakage. We confirmed the white spot was metal exposed to the exterior. These results further showcase the reliability of the TIRI method, which can effectively distinguish thermal bridges from air leakages.

7. Outlook

Looking forward, the TIRI technique has the potential to revolutionize the way building owners, contractors, and energy auditors identify air leakage sources. In the tests, the TIRI technique reaches a scan upper limit speed of about 0.2 m^2/s considering that the scan
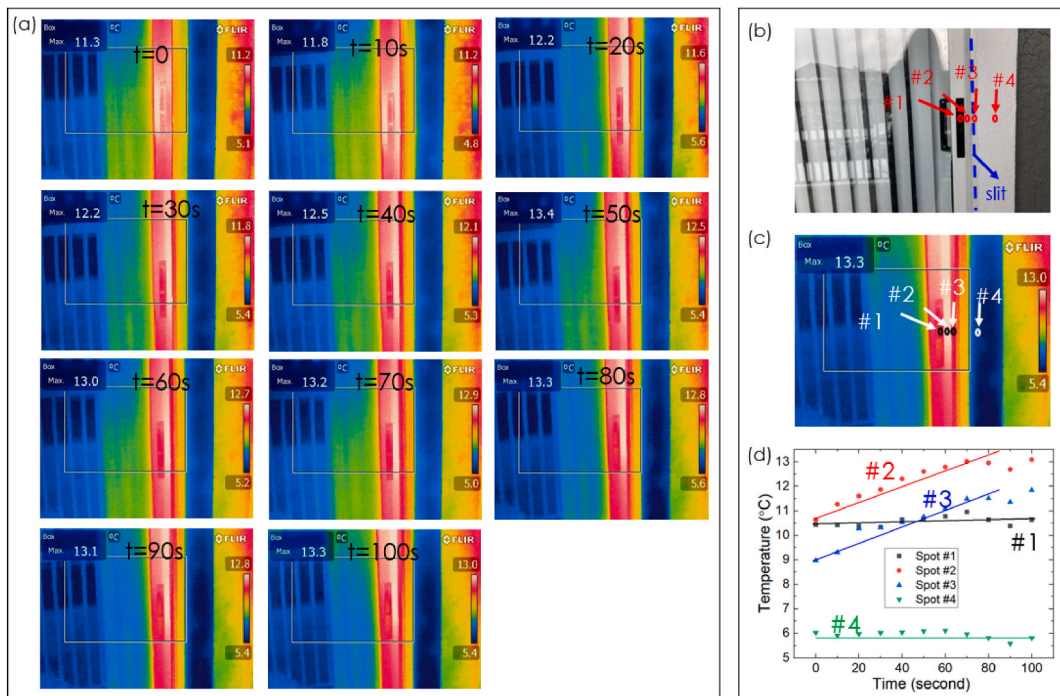

Fig. 7. Test data using the proposed TIRI method on an open-slit (1 mm) window in Salt Lake City. The locations with air leakage show clear temperature rise within a short time (100s). In contrast, the locations without air leakage show flat temperatures.
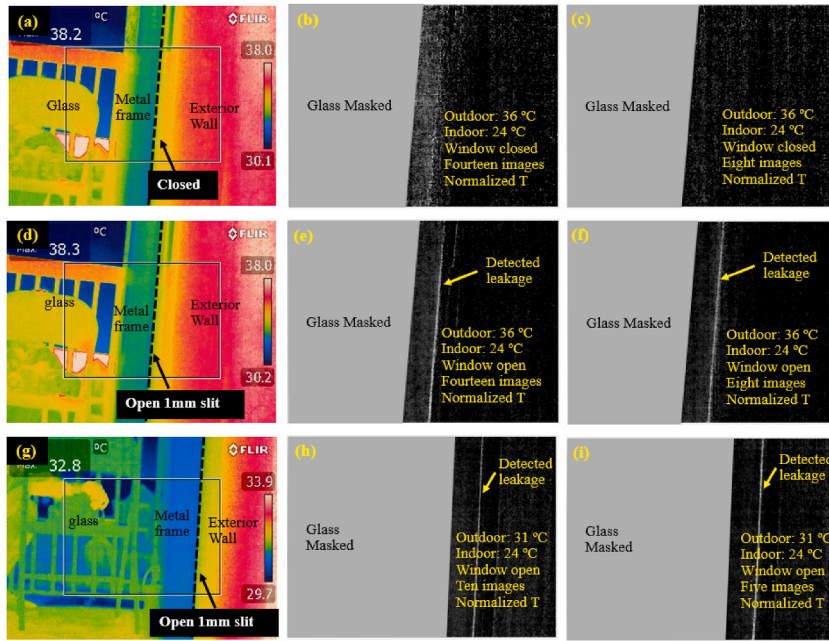
Fig. 8. Testing of the TIRI method on a closed (a–c) and open (d–i) window of a residential building in Salt Lake City at the outdoor temperature of (a–f) 36 °C and (g–i) 31 °C.
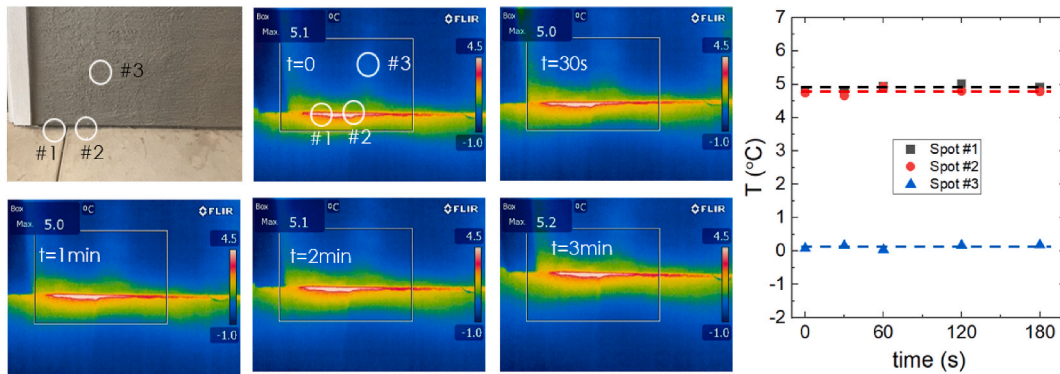

Fig. 9. Inspection of a suspicious area. In a single IR image, it looks like there is an air leakage. However, after taking transient (time-dependent) IR images, it was found that the temperatures of all spots are flat, indicating there is no air leakage. The white spot was verified to be an aluminum foil, which was just a thermal bridge. This evidence further demonstrates that our TIRI method can effectively distinguish thermal bridges from air leakages.

area is about 2 m^2 and the shortest needed scan time is 10s (with IR video fps = 30). This scan speed can be significantly improved by optimizing the image processing algorithm. The current spatial resolution, 0.5 cm^2, can also be significantly improved if a higher-resolution IR camera is used. These tests are beyond the scope of this work.

8. Conclusions

In conclusion, we have proposed and demonstrated a novel Transient IR Imaging (TIRI) method to detect the air leakages of building envelopes in different seasons and at different times of the day. We have shown that the TIRI technique can accurately and efficiently identify the leakage locations and relative rates within tens of seconds even when the indoor-outdoor temperature difference is 2 °C. Since the TIRI method does not rely on absolute temperature but on relative temperature changes, it offers a robust and high-fidelity way to detect air leakage in building envelopes. Compared to the static comparison between IR images before and after pressurization in tradition, our method is different since it tracks the transient change trajectory of temperature as a function of time. This is why our TIRI method can detect leakage within 10s, for temperature difference as small as 2 °C and works in all seasons. Since it does not require any other equipment or disrupt the inside of the buildings, it offers a simple, low-cost, portable, and non-intrusive way to detect air leakage. This work will have a broad impact in the building air leakage detection, retrofitting, and energy savings. We expect our method to accelerate the improvement of airtightness in buildings, reduce greenhouse gas emissions, and save energy for

millions of residential buildings, especially those owned by low-to-medium-income families.

Additional notes

CRediT authorship contribution statement

Tianli Feng: Writing – original draft, Validation, Supervision, Methodology, Investigation, Funding acquisition, Formal analysis, Data curation, Conceptualization. **Zhenglai Shen:** Writing – review & editing, Methodology, Funding acquisition, Conceptualization. **Som S. Shrestha:** Writing – review & editing, Methodology, Funding acquisition, Formal analysis. **Diana E. Hun:** Writing – review & editing, Supervision, Funding acquisition.

Declaration of competing interest

The authors declare the following financial interests/personal relationships which may be considered as potential competing interests. Tianli Feng, Som Shrestha, and Zhenglai Shen have patent BUILDING AIR LEAKAGE DETECTION AND QUANTIFICATION USING TRANSIENT INFRARED IMAGING pending to the University of Utah. If there are other authors, they declare that they have no known competing financial interests or personal relationships that could have appeared to influence the work reported in this paper.

Data availability

Data will be made available on request.

Acknowledgments

References

[1] U. S. Energy Information Administration, Monthly Energy Review March 2020, vol. 37, 2020.
[2] A.G. Gaglia, E.N. Dialynas, A.A. Argiriou, E. Kostopoulou, D. Tsiamitros, D. Stimoniaris, K.M. Laskos, Energy performance of European residential buildings: energy use, technical and environmental characteristics of the Greek residential sector – energy conservation and CO_2 reduction, Energy Build. 183 (2019) 86.
[3] W.R. Chan, J. Joh, M.H. Sherman, Analysis of Air Leakage Measurements from Residential Diagnostics Database, 2013.
[4] D.E. Hun, P.W. Childs, J.A. Atchley, A.O. Desjarlais, Effects from the Reduction of Air Leakage on Energy and Durability, 2013.
[5] A. Tenwolde, W.B. Rose, Moisture control strategies for the building envelope, J. Therm. Envelope Build. Sci. 19 (1996) 206.
[6] C. Harris, Opaque envelopes: pathway to building energy efficiency and demand flexibility: key to a low-carbon, Sustainable Future (2021). United States. Web. doi:10.2172/1821413.
[7] X. Zheng, J. Mazzon, I. Wallis, C.J. Wood, Airtightness measurement of an outdoor chamber using the pulse and blower door methods under various wind and leakage scenarios, Build. Environ. 179 (2020) 106950.
[8] D. Sinnott, Dwelling Airtightness, A socio-technical evaluation in an Irish context, Build. Environ. 95 (2016) 264.
[9] H. Max, M.H.S. Mhshermanlblgov, Building Airtightness: Research and Practice, 2004.
[10] F. Ascione, N. Bianco, R.F. De Masi, F. De'Rossi, G.P. Vanoli, Energy retrofit of an educational building in the ancient center of benevento. Feasibility study of energy savings and respect of the historical value, Energy Build. 95 (2015) 172.
[11] M. Mahmoodzadeh, V. Gretka, S. Wong, T. Froese, P. Mukhopadhyaya, Evaluating patterns of building envelope air leakage with infrared thermography, Energies 13 (2020).
[12] J.M. Hart, *A Practical Guide To Infra-red Thermography For Building Surveys*, Building Research Establishment 2, 1992.
[13] E. Grinzato, V. Vavilov, T. Kauppinen, Quantitative infrared thermography in buildings, Energy Build. 29 (1998) 1.
[14] M.D. Gonçalves, T. Colantonio, *Commissioning Of Exterior Building Envelopes Of Large Buildings For Resultant Moisture Accumulation Using Infrared Thermography And Other Diagnostic Tools*, Thermal Performance of the Exterior Envelopes of Whole Buildings, 2007.
[15] C.A. Balaras, A.A. Argiriou, Infrared thermography for building diagnostics, Energy Build. 34 (2002) 171.
[16] A. Kylili, P.A. Fokaides, P. Christou, S.A. Kalogirou, Infrared thermography (irt) applications for building diagnostics: a review, Appl. Energy 134 (2014) 531.
[17] T. Kalamees, Air tightness and air leakages of new lightweight single-family detached houses in Estonia, Build. Environ. 42 (2007) 2369.
[18] M.B. Dufour, D. Derome, R. Zmeureanu, Analysis of thermograms for the estimation of dimensions of cracks in building envelope, Infrared Phys. Technol. 52 (2009) 70.
[19] S. Van Den Vijver, M. Steeman, K. Carbonez, N. Van Den Bossche, V. Vaerwyckweg, On the use of infrared thermography to assess air infiltration in building envelopes, AIVC International Workshop: Quality of Methods for Measuring Ventilation and Air Infiltration in Buildings 146 (2014) 135.
[20] W. Liu, X. Zhao, Q. Chen, A novel method for measuring air infiltration rate in buildings, Energy Build. 168 (2018) 309.
[21] C. Lerma, E. Barreira, R.M.S.F. Almeida, A discussion concerning active infrared thermography in the evaluation of buildings air infiltration, Energy Build. 168 (2018) 56.
[22] M. Sherman, M. Modera, Low-frequency measurement of leakage in enclosures, Rev. Sci. Instrum. 57 (1986) 1427.
[23] P. Wahlgren, E. Sikander, *Methods And Materials For an Airtight Building*, Thermal Performance of the Exterior Envelopes of Whole Buildings - 11th International Conference, 2010.
[24] A. Casillas, M. Modera, M. Pritoni, Using non-invasive MEMS pressure sensors for measuring building envelope air leakage, Energy Build. 233 (2021) 110653.

[25] G. Raman, M. Prakash, R.C. Ramachandran, H. Patel, Remote Detection of Building Air Infiltration Using a Compact Microphone Array and Advanced Beamforming Methods, vol. 3, Berlin Beamforming Conference, 2014, p. 1.

[26] K. Chelliah, G. Raman, R.T. Muehleisen, Leakage detection techniques using nearfield acoustic holography, in: Proceedings of the ASME 2014 4th Joint US-European Fluids Engineering Division Summer Meeting, 2014, pp. FEDSM2014–21320.

[27] K. Chelliah, G.G. Raman, R.T. Muehleisen, Enhanced nearfield acoustic holography for larger distances of reconstructions using fixed parameter tikhonov regularization, J. Acoust. Soc. Am. 140 (2016) 114.

[28] G. Raman, K. Chelliah, M. Prakash, R.T. Muehleisen, *Detection And Quantification Of Building Air Infiltration Using Remote Acoustic Methods*, INTERNOISE 2014 - 43rd International Congress on Noise Control Engineering: Improving the World through Noise Control, 2014.

[29] H. Patel, K. Chelliah, G. Raman, R.T. Muehleisen, E. Tatara, Detecting building leakage using nearfield acoustic holography and a simulated crack in the building wall, in: 169th Meeting of the, Acoustical Society of America, 2015.

[30] O.A.B. Hassan, An alternative method for evaluating the air tightness of building components, Build. Environ. 67 (2013) 82.

[31] P. Boudreaux, S. Venkatakrishnan, E. Iffa, D. Hun, Application of reference-free natural background–oriented schlieren photography for visualizing leakage sites in building walls, Build. Environ. 223 (2022) 109529.

[32] T.L. Bergman, A.S. Lavine, F.P. Incropera, D.P. DeWitt, Fundamentals of Heat and Mass Transfer, eighth ed., John Wiley & Sons, Inc, 2018.

[33] T. Wong, C.W. Leung, Forced-convection augmentation of turbulent flow in a triangular duct with artificially roughened internal surfaces, Exp. Heat Tran. 15 (2002) 89.

[34] A. Bhattacharyya, Heat Transfer and Pressure Drop with Rough Surfaces, a Literature Survey, vol. 82, 1964.